Int. J. Electrochem. Sci., 14 **(2019)** 9682 – 9694, doi: 10.20964/2019.10.07

International Journal of ELECTROCHEMICAL SCIENCE
www.electrochemsci.org

Electrochemical behaviour of L-cysteine on massive chalcopyrite （$CuFeS_2$）bioleached by leptospirillum ferrooxidans

Yue Liu[1], *Hongai Zheng*[1,*], *Yiheng Zhou*[1], *Mengqian Wang*[1], *Jianshe Liu*[2], *Daquan Zhang*[1], *Lizhi Zhang*[3]

[1] College of Environmental and Chemical Engineering, Shanghai University of Electric Power
[2] 3GA 30332, United States
[3] Department of Orthopedic Surgery, ShangHai YangPu District Central Hospital, YangPu Hospital affiliated to TongJi University
[*]E-mail: zhenghongai@shiep.edu.cn

Received: 18 January 2019 / *Accepted:* 15 July 2019 / *Published:* 30 August 2019

This study introduces a mechanism for speeding up the bioleaching process. We examine the effects and kinetics of L-cysteine on the bioleaching of chalcopyrite via Potetiodynamic polarisation, electrochemical impedance spectroscopy (EIS) and cyclic voltametry tests in a Leptospirillum ferrooxidans-dominated culture. Both the polarisation curves and the EIS show that adding L-cysteine improves the bioleaching speed, but does not change the controlled step. In addition, the results of the cyclic voltametry test reveal that the anodic and cathodic current signals of the electrodes decrease. Furthermore, all the oxidation peak potentials move positively, and the oxidation peaks of the intermediate species (CuxS) persist throughout the entire bioleaching process.

Keywords: Electrochemical; Leptospirillum ferrooxidans; L-cysteine; Bioleaching; Chalcopyrite

1. INTRODUCTION

Chalcopyrite ($CuFeS_2$) accounts for approximately 70% of global copper reserves, and is commonly used to extract copper. Historically, extracting copper from chalcopyrite via pyrometallurgical means has been a conventional process. However, pyrometallurgical methods are costly in terms of capital investment, operating costs, and environmental compliance [1]. In recent years, a number of studies have proposed hydrometallurgical alternatives to conventional hydrometallurgical processes. One alternative to these processes is the bioleaching of chalcopyrite: a copper extraction process whose operation is low cost and environmentally friendly [2]. Since the end of the last century, to improve the percentage of copper extraction, researchers have used acidophilus bacteria to bioleach chalcopyrite. One extremely acidophilic bacteria (thriving at pH 2.0- 3.0) is L. ferrooxidans; This bacteria is usually regarded as mesophilic [3]. It carries out bio-oxidation at 40℃ or less, and it grows

only by aerobically oxidizing iron (II) ions. Many scholars [4-6] have found that using L. ferrooxidans not only improves the leaching kinetics of chalcopyrite, but also hinders passivation.

The main problems associated with chalcopyrite bioleaching are that leaching is slow and often incomplete [7]. Most researchers have suggested that the low chalcopyrite dissolution rate is rooted in a passivation layer that forms on the chalcopyrite surface, such as metal-deficient sulphides, elemental sulphur, polysulphides, jarosites, and extracellular polymeric substance (EPS) [8]. The passivation layer may cover the chalcopyrite surface, which restricts the flow of bacteria and oxidants to further oxide chalcopyrite, thus hampering copper extraction [9, 10]. Studies have already revealed that increasing bacterial activity or changing the surface property of the minerals could improve bioleaching performance [11]. According to these reports, adding L-histidine, L-glutamic acid, L-methionine, L-aspartic acid, or yeast extract can improve the bioleaching rate [12]. A study conducted by Hu Y [13] has proven that adding a suitable amount of L-cysteine can facilitate the bioleaching of pyrite via Acidithiobacillus ferrooxidans. Rojas Chapana and Tributsch [11], for example, enhanced the leaching of sphalerite by adding L-cysteine via Acidithiobacillus ferrooxidans. He Z [14] has further found that adding a suitable mass of L-cysteine was favourable for nickel-copper sulphide leaching via Acidithiobacillus caldus or Acidianus manzaensis [15]. Wang Z [16] has also noted that cysteine has a chemisorption effect on pyrite surfaces, and that adding cysteine makes pyrite more liable to be oxidized, even at a lower potential. However, adding L-cysteine to improve the bioleaching rate of chalcopyrite was rarely reported, and therefore the mechanism related to L-cysteine remains unclear. Understanding the mechanism involved in this process can aid in finding cheaper additives to enhance the bioleaching rate.

In this study, we use Potetiodynamic polarisation, EIS and cyclic voltametry to characterise the dissolution of Cu during bioleaching, using massive chalcopyrite electrodes and Leptospirillum ferrooxidans (L. f). Furthermore, we evaluate the effects of L-cysteine on chalcopyrite bioleaching. During bioleaching, we observe the surface of the chalcopyrite electrode using an optical microscope.

2. MATERIALS AND METHODS

2.1. Chalcopyrite

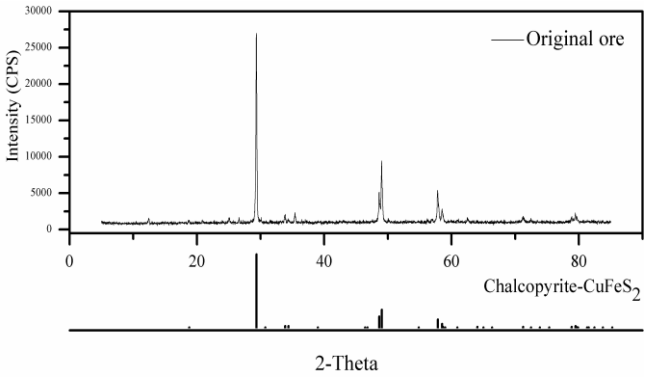

Figure 1. Results of XRD spectrum of chalcopyrite

The chalcopyrite used in this work was obtained from the mineral museum in Hubei, China. A quantitative X-ray diffraction analysis revealed that the only crystalline phase present in the sample was chalcopyrite (94.5 wt%). The mass percentage of each element in the chemical analysis of the pure mineral samples was 32.51% Cu, 31.92% Fe, and 33.47% S.

2.2. Microorganisms and growth conditions

This study used strains of L. ferrooxidans (DQ343299) that were provided by the Key Laboratory of Biometallurgy at Central South University in Changsha, China. The bacteria were cultivated in medium ($FeSO_4$•$7H_2O$ (44.2 g/L) $(NH_4)_2SO_4$ (3.0 g/L), K_2HPO_4(0.5 g/L), $MgSO_4$•$7H_2O$ (0.5 g/L), KCl (0.1 g/L), $Ca(NO_3)_2$(0.01 g/L)), and with a rotary shaker. The initial pH value of the L. ferrooxidans in the aforementioned solution was 2.0. The temperature of the rotary shaker was controlled at 40°C, and its rotating speed was 180r/min. When the bacteria reached the logarithmic growth phase, the culture was centrifuged in a separator at 5,000rpm for 5min to remove impurities from the culture, and then centrifuged again at 14,000rpm for 20min to separate the supernatant from the culture. The resulting white precipitate on the bottom is the aggregate of the bacteria. The centrifuged bacteria were washed with sterilised diluted sulphuric acid with a pH of 1.6. The washing and centrifugation steps were repeated three times until the cells were free from the precipitates. For the following experiments, we used a Fe^{2+} free medium to dilute the white precipitate to 2×10^7 cells/ml of the bacterial suspension.

2.3 The Electrochemical Study

The working electrodes were prepared by cutting samples of chalcopyrite with a surface of approximately 1 cm2 and polishing them with an emery board so that there were no visible imperfections. A copper wire was connected by soldering tin on its back face. The exposed surface of mineral electrode was polished by 600# sand paper and rinsed by double-distilled water. The electrochemical measurements were conducted in a three-electrode system composed of a counter electrode (platinum), working electrode (chalcopyrite), and a reference electrode (SCE). The electrochemical experiments were conducted at 40°C using a Chenhua 660C Potentiostat (China) with Chi660c software.In the Cyclic Voltammetry experiment, we modulated apositive-going potential scan from 0 to 600 mV, a negative-going potential scan from 600 to 800 mV, and a positive-going potential scan from -800 to 0 mV. All tests were scanned at a rate of 20mV/s. In another experiment, the Tafel curves were scanned from −300 mV to +1100 mV at a rate of 1 mV/s. In addition, EIS tests were conducted under open circuit potential in a frequency range of 10^{-1} to 10^5Hz with a peak-to-peak amplitude of 5 mV.

3. RESULTS AND DISCUSSION

3.1. Microscopy of chalcopyrite electrode surface

The micro graphs shown in Figure 2 (A–D) present the surface morphology of chalcopyrite electrodes after bioleaching for 0, 3, 5, and 10 days. The micrographs exhibit marked changes of morphology on the surface of the chalcopyrite that occurred during the bioleaching experiments. As the bioleaching time of the chalcopyrite electrode increased, the degree of corrosion of the chalcopyrite electrode surface became more significant. On day five (Figure 2C), corrosion products were observed on the surface of the chalcopyrite electrodes. After three days of leaching, the chalcopyrite had already begun to corrode (Figure 1 B, C, and D).

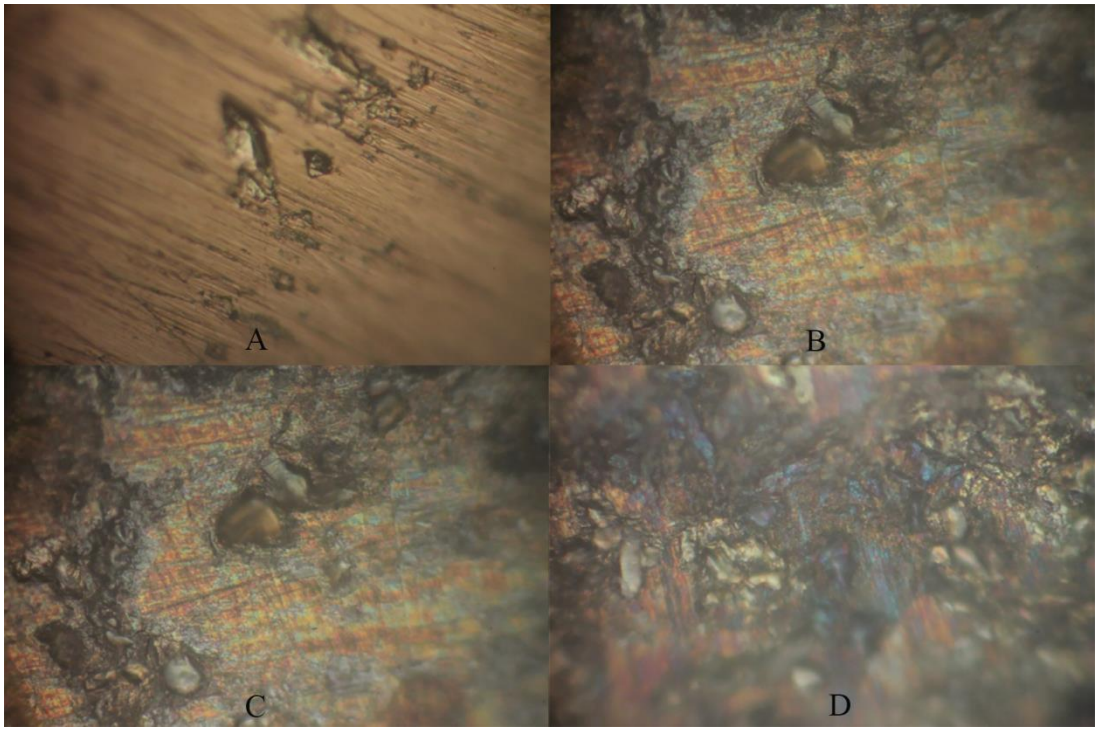

Figure 2. The surface morphology of original chalcopyrite electrode and bioleaching for three, five, and ten days.

3.2 Potentiodynamic polarisation measurements

The polarisation curve was used to identify and compare the corrosion situation of the chalcopyrite electrodes immersed in different concentrations of L-cysteine—with and without bacteria—in an iron-free medium for 12 hours. Then, a suitable amount of L-cysteine was added to the iron-free medium bioleaching of the chalcopyrite electrodes for 3, 5, and 10 days, respectively. Figures 3 and 4 illustrate the Potentiodynamic polarisation curves. Tables 1 and 2 depict the corrosion current density (icorr) and the corrosion potential (Ecorr) of the chalcopyrite electrodes under different experimental conditions.

Figure 3 reveals that the potentiodynamic curves shift to more positive potentials in the presence of cysteine. The anodic regions of the polarisation curves were similar when the electrode potential was lower than 0.3 V vs SCE. For higher electrode potentials, the anodic current density increased with increasing cysteine concentration. The effect of cysteine on the current density observed on the dissolution current density values is reported in Table 1. From Table 1, it can also be seen that no linear relationship exists between the bioleaching rate and the L-cysteine concentration, although an increasing trend can be seen in the current density, corresponding to an increase in cysteine concentration (up to a concentration of 10-3M in the presence of L.f), which indicates that adding a certain amount of L-cysteine substantially enhances the activity of L. ferrooxidans. We also find that the icorrs of the chalcopyrite electrodes with 10-3M L-cysteine without strains is the lowest, at only 3.7μA. Moreover, the icorrs of the chalcopyrite electrodes without L-cysteine that contain strains (L.f) are higher than those without strains. In addition, the icorrs of the chalcopyrite electrodes that contain both strains (L.f), and those of L-cysteine are higher than the icorrs that contain strains without L-cysteine. Thus, L-cysteine also enhances bioleaching efficiency. However, it should be noted that the transfer coefficient and number of electron transfer—both of which are indicative of electrode reaction mechanism—did not obviously change in the absence and presence of cysteine. This suggests that the addition of cysteine facilitates the electron transfer, but does not change the chalcopyrite oxidation mechanism [17]. L-cysteine, which contains –HS groups, is used as a substrate or a reduced sulphur source for organisms [11]; –HS groups also can combine with a metal to accelerate electron transfer, and thus enhance the bioleaching rate. Therefore, cysteine may serve as a bridge or conductor to facilitate electronic charge transfer from chalcopyrite and end-product. Previous studies have shown that bridge complexes formed by adsorbing ⁻O⁻, ⁻CN⁻ or ⁻CO⁻ groups to interfacial iron atoms in chalcopyrite could greatly accelerate the transfer of charge carriers between chalcopyrite and soluble iron.

In this paper, we experimented on four concentrations to select an optimal L-cysteine concentration (10^{-3}M) for future work.

Table 1. Electrochemical corrosion parameters of chalcopyrite electrode bioleaching for 12h

Strains	Sterile	L.f	L.f	Sterile	L.f	L.f	L.f
L-cysteine(mol·L^{-1})	0	0	10^{-2}	10^{-3}	10^{-3}	5×10^{-4}	10^{-4}
icorr(μA·cm^{-2})	6.3	7.5	7.8	3.7	13.9	11.6	11.0
Ecorr(mV)	210	225	248	147	253	257	247
βc(mV/dec)	35	45	44	41	30	37	37
βa(mV/dec)	65	48	50	95	53	51	56

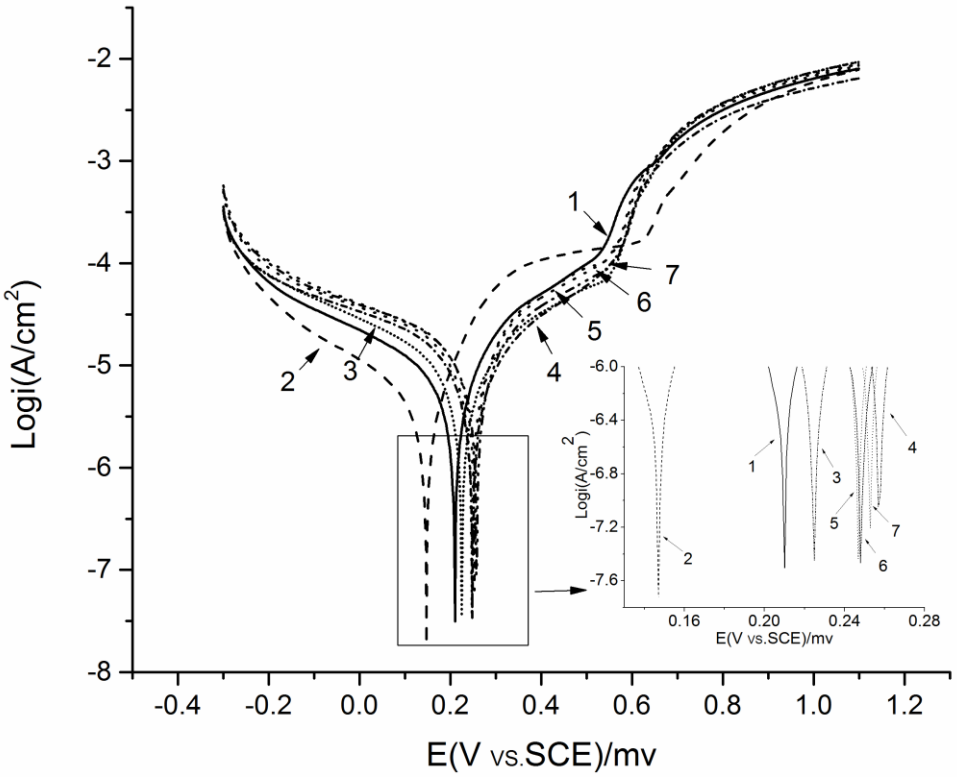

Figure 3. Potentiodynamic polarization curves for chalcopyrite electrode bioleaching for 12h by L. ferrooxidans with differential L-cysteine concentration in a 9k iron-free medium（1- 0M L-cysteine, sterile; 2- 0ML-cysteine, L.f;3- 10^{-3}M L-cysteine, sterile; 4- 10^{-2}M L-cysteine, L.f; 5- 10^{-3}M L-cysteine, L.f; 6- 5×10^{-4}M L-cysteine, L.f; 7- 10^{-4}M L-cysteine, L.f）

Table 2 shows the corrosion current density (icorr) and corrosion potential (Ecorr) of chalcopyrite electrode bioleaching after the addition of L-cysteine (10^{-3}M) iron-free medium. From Table 2 and Figure 4, it can be seen that in the mixed bacteria system with 10^{-3} M L-cysteine, the self-corrosion potential of the chalcopyrite electrode was within the range of 180.0-207.0mv, and the change in corrosion potential was not significant. The corrosion current density increased continuously from the third day to the tenth day, and reached a maximum value of 87.2μA·cm^{-2} on the tenth day. We can thus conclude that, with the increase of immersion time, icorr increases and Ecorr decreases. The data demonstrate that, with the passage of time, the corrosion of chalcopyrite electrodes increases, indicating that the chalcopyrite decomposition rate increases with time.

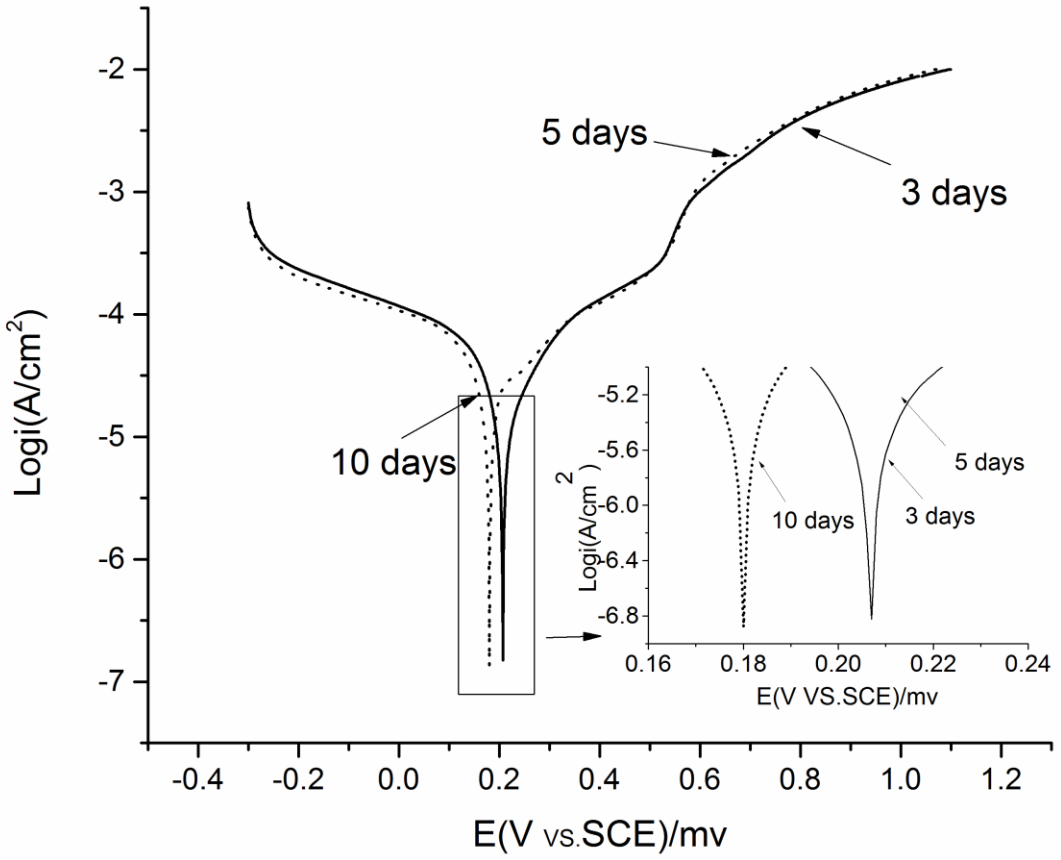

Figure 4. Potentiodynamic polarization curves for chalcopyrite electrode bioleaching for three days, five days, and ten days by L. ferrooxidans with certain concentration of L-cysteine(10-3M) in 9k iron-free medium

Table 2. Electrochemical corrosion parameters of chalcopyrite electrode at different immersion time

Time(days)	3	5	10
Strains	L.f	L.f	L.f
L-cysteine(mol·L^{-1})	10^{-3}	10^{-3}	10^{-3}
i_{corr}(μA·cm^{-2})	45.1	47.8	87.2
E_{corr}(mV)	207	204	180
βc(mV/dec)	37	37	32
βa(mV/dec)	34	34	24

3.3. Electrochemical impedance spectroscopic measurements

In recent years, the electrochemical impedance spectroscopy was widely used to analysis the adsorption and the film formation process in corrosion system. The parameters of spectroscopy of

electrochemical impedance are quite useful for analysing a corrosive mechanism [17]. In this study, we used EIS to conduct a preliminary research on mineral/solution interface structure changes. Figure 5 illustrates the EIS plot of chalcopyrite electrodes under various experimental conditions in the iron-free medium for 12 hours.

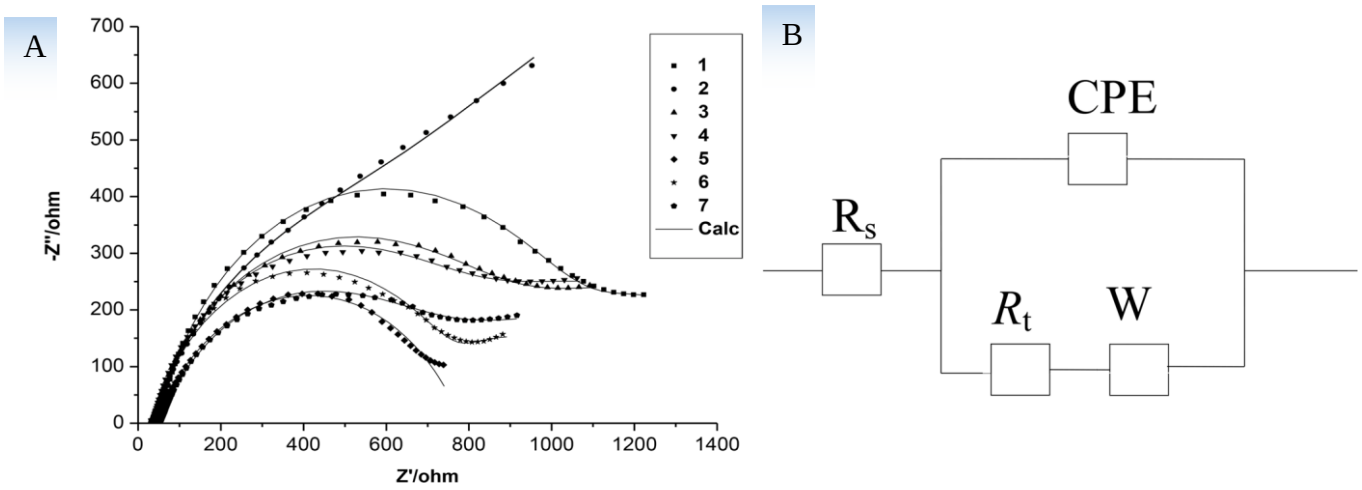

Figure 5. EIS plot (A) and an equivalentcircuit (B) for chalcopyrite electrode bioleaching for 12h by L. ferrooxidanswith a differential L-cysteine concentration in a 9k iron- free medium（1- 0M L-cysteine, sterile; 2- 0M L-cysteine, L.f;3- 10^{-3}M L-cysteine, sterile; 4- 10^{-2}M L-cysteine, L.f; 5- 10^{-3}M L-cysteine, L.f; 6- 5×10^{-4}M L-cysteine, L.f; 7- 10^{-4}M L-cysteine, L.f）

Table 3. Electrochemical impedance spectroscopy data of chalcopyrite electrode in medium in presence of L.fand differential L-cysteine concentration

EIS parameter / system	Rs(Ω·cm^2)	n	Rt(Ω·cm^2)
1- 0M L-cysteine, sterile	49.54	0.83	1040.00
2- 0M L-cysteine, L.f	33.15	0.77	905.60
3- 10^{-3}M L-cysteine sterile	37.32	0.77	925.40
4- 10^{-2}M L-cysteine, L.f	33.41	0.78	835.00
5- 10^{-3}M L-cysteine, L.f	31.98	0.79	725.80
6- 5×10^{-4}M L-cysteine, L.f	34.19	0.78	741.80
7- 10^{-4}M L-cysteine, L.f	43.37	0.75	757.40

Figure 5 shows the effect of cysteine on the complex impedance plots of the $CuFeS_2$ electrode. A general decrease in the overall impedance can be observed with an increasing cysteine concentration (up to 10^{-3}M) in the presence of L.f. Further increases in cysteine concentration resulted in an increase in the impedance, in agreement with the results observed in Figure 3. All curves exhibit an arc in the high-frequency region, and an oblique line in the low-frequency region. This suggests that the oxidation

reaction is controlled by the electron transfer step in the high-frequency region, and is diffusion-controlled in the low-frequency region. In addition to this, an inductive loop was observed in the low-frequency region, possibly related to the presence of an adsorbed species on the surface of the electrode. All of the curves indicate that the addition of L-cysteine does not change the controlled step of bioleaching [18]. Figure 5A reveals that the arc is largest without L. ferrooxidans and L-cysteine. After the addition of the bacteria and L-cysteine, the arc decreases by several degrees, and when the L-cysteine concentration is 10^{-3}M, the arc is smallest. Thus, we can infer that the speed of the chalcopyrite bioleaching accelerates with the addition of L-cysteine, which is consistent with the Tafel conclusion.

The use of equivalent electrical circuits (EEC) is a common approach to fit EIS experimental data. The EEC used is presented in Figure 5B. It depicts the equivalent circuit model, which consists of a charge transfer resistance (Rt); a solution resistance (Rs) and a constant phase element (CPE) that substitutes for the capacitor of the double-layer; and a Warburg impedance (W), which represents the diffusion impedance of the reaction products. We can see that the equivalent circuit is consistent with the electrochemical impedance spectroscopy, meaning that, in the presence of L. ferrooxidans, the selected equivalent circuit can reflect the electro-chemistry behaviour of chalcopyrite.

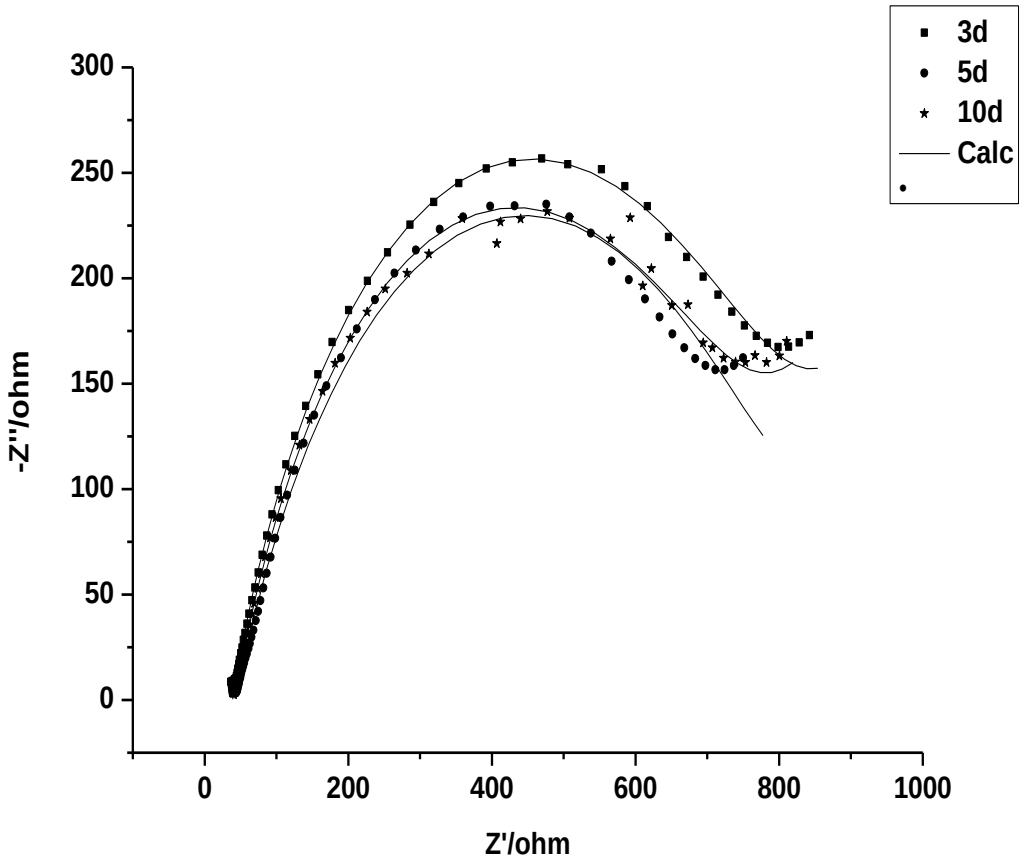

Figure 6. EIS plot for chalcopyrite electrode bioleaching for 3days, 5days, 10days by L. ferrooxidans with a certain concentration of L-cysteine (10^{-3}M) in iron free medium

Table.4 Impedance parameters of chalcopyrite electrode bioleaching for 3days, 5days, 10days in presence of L.f and 10^{-3} M L-cysteine

EIS parameter / Bioleaching time(days)	Rs(Ω·cm^2)	n	Rt(Ω·cm^2)
3	26.19	0.67	714.20
5	22.33	0.68	599.20
10	23.57	0.74	486.70

Figure 6 illustrates the EIS of chalcopyrite electrode as a function of reaction time with L. ferrooxidans and L-cysteine (10^{-3}mol·L-1). From figure 6, we also find that at high frequency there is an arc. Conversely, at a low frequency, an oblique line appears, which demonstrates that, at a high frequency, the electron transfer step controls the oxidation reaction and, at low frequency, diffusion controls the reaction. On the tenth day, the EIS arc is slightly smaller than on the fifth day. The electrode surface may be covered by a passive film, which slows down the dissolution rate of the chalcopyrite. The equivalent circuit model was the same as in Figure 5B. From figure 6 it is evident that an equivalent circuit is consistent with the electrochemical impedance spectroscopy.

3.4 Cyclic voltammetry studies

Before bioleaching the chalcopyrite electrodes with L-cysteine (10^{-3}M), we performed cyclic voltametry tests (Figure 7A). Figure 7 B–D reveal the influence of time on the cyclic voltammograms of chalcopyrite electrodes when L. ferrooxidans and L-cysteine (10^{-3}M) are added. The results indicate that adding L. ferrooxidans and L-cysteine (10^{-3}M) does not change the mechanisms of oxidative and reductive reaction of the chalcopyrite electrodes.

There are three anodic peaks (A1, A2, and A3) and four cathodic peaks (C1, C2, C3, and C4), as shown in Figure 7. According to Klauber et al. [19], the products of chalcopyrite in bioleaching are elemental S^0, CuS, and Fe^{2+}. Biegler and Horne [20] and Gómez [21] have found that the A2 process indicates that the chalcopyrite was oxidated, as shown in Equations (1) and (2).

$$CuFeS_2 \leftrightarrow Cu_{1-x}Fe_{1-y}S_{1-z} + xCu^{2+} + yFe^{2+} + zS + 2(x+y)e^- \quad (1)$$

$$CuFeS_2 \leftrightarrow 0.75CuS + 1.25S + 0.25Cu^{2+} + Fe^{2+} + 2.5e^- \quad (2)$$

According to Gómez [21], López-Juárez [22] and Liang [23], Peak A3 indicates that the massive chalcopyrite dissolved and that the covellite had been decomposed to elemental sulphur, copper ions, and/or sulphate, as shown in Equations (3)–(5).

$$CuFeS_2 \leftrightarrow 2S^0 + Cu^{2+} + Fe^{3+} + 5e^- \quad (3)$$

$$CuFeS_2 + 8H_2O \leftrightarrow Cu^{2+} + Fe^{3+} + 2SO_4^{2-} + 16H^+ + 17e^- \quad (4)$$

$$CuS + 4H_2O \leftrightarrow Cu^{2+} + SO_4^{2-} + 8H^+ + 8e^- \quad (5)$$

The inverse scan reduction peaks C1 and C2 are attributed to ferric and copper ion reduction, according to Equations.(6)–(8) [24]

$$Fe^{3+} + e^- \leftrightarrow Fe^{2+} \quad (6)$$

$$Cu^{2+} + S^0 + 2e^- \leftrightarrow CuS \quad (7)$$

$$Cu^{2+} + 2e^- \leftrightarrow Cu^0 \quad (8)$$

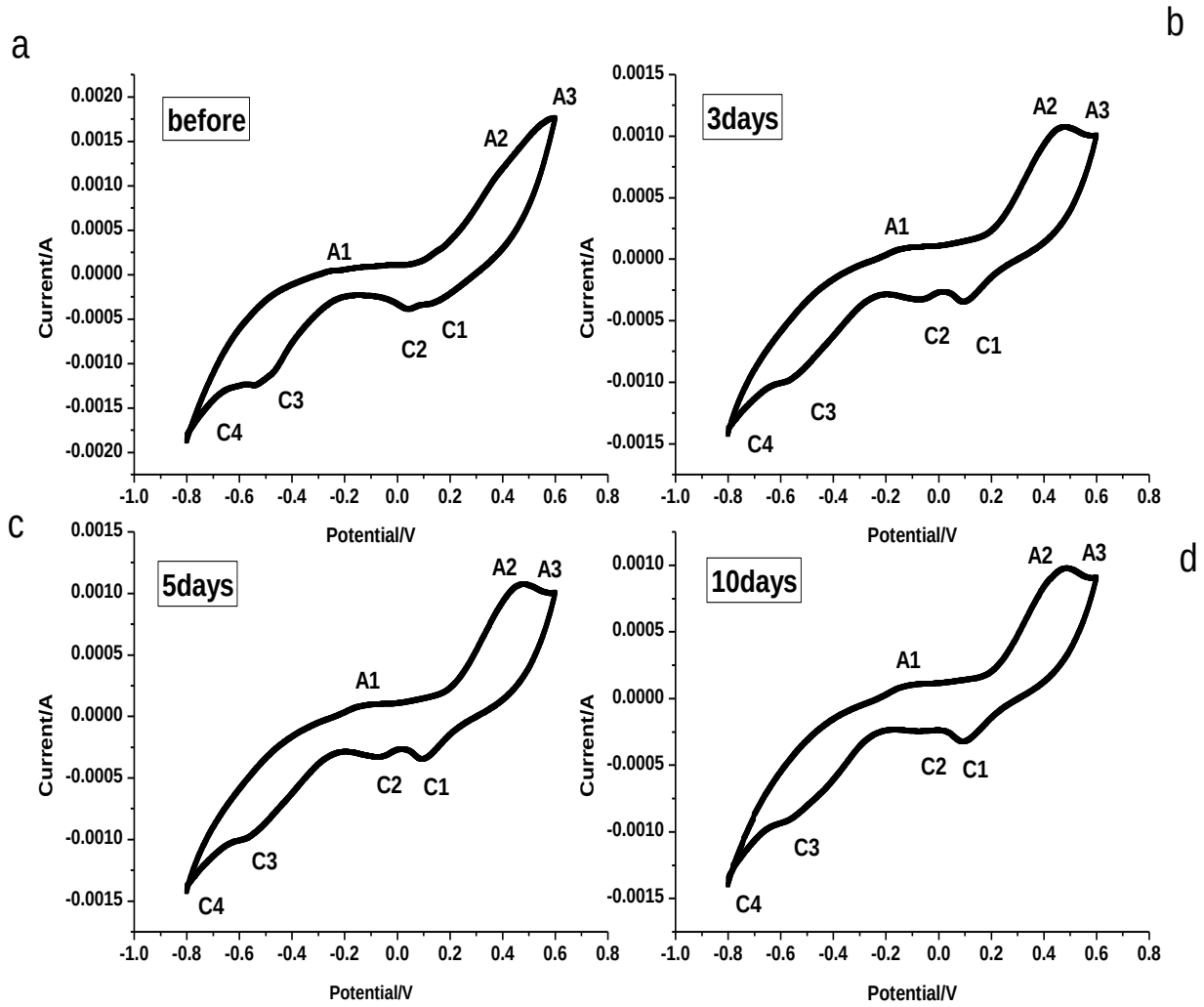

Figure 7. Cyclic voltammograms of chalcopyrite electrodes before bioleaching and bioleached for 3, 5, 10 days by L. ferrooxidans with certain concentration of L-cysteine (10^{-3}M) in iron free medium.

According to Gonzalez [25] and Arce [10], peaks C3 and C4 are caused by a reduction of covellite and chalcopyrites, as shown in Equations (9) and (10).

$$2CuS + 2H^+ + 2e^- \leftrightarrow Cu_2S + H_2S \quad (9)$$

$$2CuFeS_2 + 6H^+ + 2e^- \leftrightarrow Cu_2S + 2Fe^{2+} + 3H_2S + e^- \quad (10)$$

According to the cathodic reaction shown above, peak A1 may be caused by the oxidation of copper (Equation (11)) [24]

$$2Cu + HS^- + OH^- \leftrightarrow Cu_2S + H_2O + 2e^- \quad (11)$$

From Figure 7 B–D, we can draw the following conclusions: Throughout the entire bioleaching process, the product always exists on the electrode surface. After bioleaching, the cathodic and anodic currents decrease. This decrease in current is mainly caused by the passivation layer which is formed on the surface of the chalcopyrite electrodes. Furthermore, in our work, during bioleaching, all of the

oxidation peak potentials moved positively, indicating that a higher potential is needed to oxidize the chalcopyrite during the bioleaching process, likely due to the formation of a passivation layer on the surface of the electrodes. When the L-cysteine with certain concentration of 10-3M is added, the valence changes of Cu and S in chalcopyrite are still between Cu^0 and Cu^{+2}, and between S^{-2} and S^0[2]. These changes in valence state will produce various types of intermediates, such as CuO, Cu_2O, $Cu_{1-x}Fe_{1-y}S_{1-z}$[11]. The intermediates formed a passivation film on the surface of chalcopyrite electrode with extracellular polymers and jarosite and other substances under inappropriate oxidation conditions[26]. When the L-cysteine with certain concentration of 10^{-3}M is added, L-cysteine reacted with the intermediates, resulting in the reduce of the production of passivation film and the accelerate of the dissolution of chalcopyrite[27].

According to the electrochemical measurement results, it can be found that the dissolution characteristics of massive chalcopyrite electrodes in an L. Ferrooxidans system with the addition of L-cysteine. Potentiodynamic polarisation measurements showed that with the passage of time, the corrosion of chalcopyrite electrodes increases, indicating that the chalcopyrite decomposition rate increases with time. Electrochemical impedance spectroscopic indicated that electrode surface may be covered by a passive film, which slows down the dissolution rate of the chalcopyrite. We further proposed that the dissolution mechanism of massive chalcopyrite electrodes in an L. Ferrooxidans system with the addition of L-cysteine. In single chalcopyrite leaching system, the surface of chalcopyrite electrode formed a thicker layer of passivation film, lead to the low anode and the cathode electrode current. When the L-cysteine with certain concentration of 10-3M is added, the L-cysteine significantly decrease the chalcopyrite electrode surface passivation membrane, promote the dissolution of chalcopyrite.

4. CONCLUSION

This study employed electrochemical methods to investigate the dissolution characteristics of massive chalcopyrite electrodes in an L. Ferrooxidans system with the addition of L-cysteine. The potentiodynamic polarisation and EIS results reveal that the concentration of L-cysteine increases corrosion current density and corrosion potential of the chalcopyrite, although it does not change the controlled step of bioleaching. An analysis of the cyclic voltammetry curve indicates that adding L-cysteine improves the speed of bioleaching, but does not change the controlled step of bioleaching. On the tenth day of bioleaching, the passivation layer began to form on the chalcopyrite surface, a decrease in the bioleaching rate.

References

1. T. Naseri, N. Bahaloo-Horeh and S. M. Mousavi, *J. Environ. Manage.,* 235 (2019) 357.
2. Y. Huang, *Int. J. Electrochem. Sci.,* 12 (2017) 10493.
3. H. Liu, X. Lu, L. Zhang, W. Xiang, X. Zhu, J. Li, X. Wang, J. Lu and R. Wang, *Chem. Geol.,* 493 (2018) 109.

4. L. Cancho, M. L. Blázquez, A. Ballester, F. González and J. A. Muñoz, *Hydrometallurgy,* 87 (2007) 100.
5. H. B. Zhou, W. M. Zeng, Z. F. Yang, Y. J. Xie and G. Z. Qiu, *Bioresour. Technol.,* 99 (2009) 515.
6. Z.-j. Yu, R.-l. Yu, A. j. Liu, J. Liu, W.-m. Zeng, X.-d. Liu and G.-z. Qiu, *Trans. Nonferrous. Met. Soc.,* 27 (2017) 406.
7. J.-l. Xia, J.-j. Song, H.-c. Liu, Z.-y. Nie, L. Shen, P. Yuan, C.-y. Ma, L. Zheng and Y.-d. Zhao, *Hydrometallurgy,* 180 (2018) 26.
8. K. Harneit, A. Göksel, D. Kock, J. H. Klock, T. Gehrke and W. Sand, *Hydrometallurgy,* 83 (2006) 245.
9. R. P. Hackl, D. B. Dreisinger, E. Peters and J. A. King, *Hydrometallurgy,* 39 (1995) 25.
10. A. F. Tshilombo, J. Petersen and D. G. Dixon, *Miner. Eng.,* 15 (2002) 809.
11. J. A. Rojas-Chapana and H. Tributsch, *Process Biochem.,* 35 (2000) 815.
12. O. G. Olvera, P. Valenzuela, D. G. Dixon and E. Asselin, *Hydrometallurgy,* 169 (2017) 552.
13. Y. Hu, Z. He, W. Hu, H. Peng and H. Zhong, *Trans. Nonferrous. Met. Soc.,* 14 (2004) 794.
14. Z. He, F. Gao, Z. Hui and Y. Hu, *Bioresour. Technol.,* 99 (2009) 1383.
15. Z. He, J. Zhao, W. Liang, Y. Hu and G. Qiu, *J. Cent. South Univ.,* 18 (2011) 381.
16. Z. Wang, X. Xie, S. Xiao and J. Liu, *Hydrometallurgy,* 101 (2010) 88.
17. P. L. Bonora, F. Deflorian and L. Fedrizzi, *Electrochim. Acta,* 41 (1996) 1073.
18. X. C. Zhang, S. B. Wei, H. M. Yuan and Y. Jin, *J. Anhui Agri. Univ.,* 37 (2010) 51.
19. C. Klauber, A. Parker, W. v. Bronswijk and H. Watling, *Int. J. Miner. Process.,* 62 (2001) 65.
20. T. Biegler and M. D. Horne, *J. Electrochem. Soc.; (United States),* 132 (1985) 1363.
21. C. Gómez, M. Figueroa, J. Muñoz, M. L. Blázquez and A. Ballester, *Hydrometallurgy,* 43 (1996) 331.
22. A. López-Juárez, N. Gutiérrez-Arenas and R. E. Rivera-Santillán, *Hydrometallurgy,* 83 (2006) 63.
23. C. L. Liang, J. L. Xia, Y. Yang, Z. Y. Nie, X. J. Zhao, L. Zheng, C. Y. Ma and Y. D. Zhao, *Hydrometallurgy,* 107 (2011) 13.
24. W. Zeng, G. Qiu, H. Zhou and M. Chen, *Hydrometallurgy,* 105 (2010) 259.
25. E. M. Arce and I. González, *Int. J. Miner. Process.,* 67 (2002) 17.
26. J. Y. Zhu, P. YANG, B.-m. LI, J.-x. ZHANG and Q.-x. HUANG, *Trans. Nonferrous Met.Soc,* 18 (2008) 1439.
27. y. Hu, z. He, w. Hu, h. Peng and h. Zhong, *Trans. Nonferrous Met.Soc,* 14 (2004) 794.